POAC'25
St. John's, Newfoundland and Labrador, Canada

Proceedings of the 28th International Conference on Port and Ocean Engineering under Arctic Conditions
Jul 13-17, 2025
St. John's, Newfoundland and Labrador
Canada

Parametric Analysis of Ship-Ice Dynamic Interaction Scenarios Based on FEM

Wenlong Li[1], Li Zhou[1], Pentti Kujala[1,2], Shixiao Fu[1], Guangwei He[3], Feng Diao[4], Fang Li[1]

[1] State Key Laboratory of Ocean Engineering, Shanghai Jiao Tong University, Shanghai, China

[2] Estonian Maritime Academy, Tallinn University of Technology, Tallinn, Estonia

[3] Guangzhou Shipbuilding International Co., Ltd., Guangzhou, China

[4] China Ship Scientific Research Center, Wuxi, China

ABSTRACT

In polar regions, the bows of ships and offshore structures are typically designed with inclined surfaces to induce bending failure in sea ice and reduce the loads acting on the structures. The most widely used analytical model for analyzing the bending behavior of sea ice to date is the wedge beam assumption. However, in real ice conditions encountered by icebreaking vessels, the ice sheet more closely resembles a wedge-shaped ice body connected to a semi-infinite ice sheet. The geometric simplification of the wedge beam may lead to inaccuracies in estimating the stress distribution within the ice. Additionally, most current studies are based on quasi-static conditions, where the contact force is typically assumed to act over a fixed area, and the process of force application moving with time is often neglected. As a result, it is difficult to consider dynamic effects during ship–ice interactions. Furthermore, previous studies have often neglected the influence of in-plane forces and friction forces in the horizontal direction. This study aims to re-parameterize the geometric representation of ice sheet in ship–ice interaction scenarios. To represent the penetration process more accurately during local ship–ice interaction, a user-defined subroutine is implemented to apply the pressure load at a position that evolves over time with Finite Element Method (FEM). A parametric analysis was conducted to investigate the influence of the re-parameterized variables on the stress experienced by the ice and the location of the maximum stress. The results of this study provide valuable insights into the mechanics of ship-ice interactions.

KEY WORDS: Ice Wedge; Ship-ice Interaction; Dynamic bending; Ice force; Finite Element Method.

INTRODUCTION

Sea ice covers the majority of polar regions. While thick and solid ice can serve as offshore roads and airstrips, it also brings significant risks to polar ships and marine structures. This study focuses on the latter. In the interaction between sea ice and ships or offshore structures, the strength of the ice determines the magnitude of the ice load imposed on the structure. Since the flexural strength of sea ice is generally lower than its compressive strength, the bows of polar ships and offshore structures are typically designed with inclined surfaces. This design allows the structure to exert a vertical bending force to the ice through the inclined surface, making it easier to break the ice and thereby reducing the ice load.

Over the past few decades, various methods have been developed to predict the ice loads during the interaction between ice and structures. These include analytical solutions based on the wedge beam assumption (e.g., Kerr, 1976; Nevel, 1961), numerical solutions based on simulation methods (e.g., Lubbad and Løset, 2011; Metrikin and Løset, 2013), and empirical formulas based on experimental data (Lindqvist, 1989; Riska et al., 1997). Among these, analytical models serve as the foundation for the other research methods. Nevel (1961) proposed the narrow wedge beam model on an elastic foundation, which is one of the most widely applied analytical models in ship-ice interaction problems. Subsequent researchers have carried out numerous studies based on this foundation (Varsta, 1983; Li et al., 2019).

However, in the actual interaction between ships and sea ice, the shape of the ice is not a narrow wedge-shaped beam. Zhou et al. (2018) observed that during ship-ice interactions, the failure of sea ice is primarily characterized by circumferential cracking. Therefore, the ice sheet is more accurately like a wedge connected to a semi-infinite ice cover. The failure that occurs during the interaction between the ice sheet and the inclined structure can be viewed as the result of multiple localized bending failures within the ice sheet. This geometric simplification in Nevel's narrow wedge-shaped beam model may result in inaccuracies in estimating the stress distribution within the ice sheet.

Moreover, in previous studies, the interaction force between the ship and sea ice was typically simplified as a bending force (i.e., out-of-plane force) applied over a fixed area, while the effects of in-plane forces and friction forces were often neglected. The influence of variations in the position of force application was also overlooked in these models. Li et al. (2024) pointed out that in-plane forces and loading speed can enhance the bearing capacity of an ice wedge.

This study aims to parameterize the ship-ice interaction scenario more accurately and establish a local interaction model between the ship and the ice. Based on Finite Element Analysis (FEA), this study investigates the influence of these parameters on the stress distribution within the ice.

METHODS

Simplification and parameterization of ship-ice interaction scenarios

Based on the analysis presented in Section 1, the ice sheet in this study is simplified as an ice wedge connected to a semi-infinite ice plate, as shown in Figure 1. The edge of the ice wedge is arc-shaped and tangent to the bottom edge of the ice sheet. The shape of the ice wedge can be characterized by two main parameters: the wedge depth b and the wedge angle θ.

Nevel (1961) demonstrated that an ice wedge on an elastic foundation can be nondimensionalized using the characteristic length l_c:

$$l_c = \left(\frac{Eh^3}{\rho_w g}\right)^{\frac{1}{4}} [m] \quad (1)$$

Where E is the elastic modulus of sea ice, h is the thickness of the ice sheet, ρ_w is the density of seawater, and g is the gravitational acceleration.

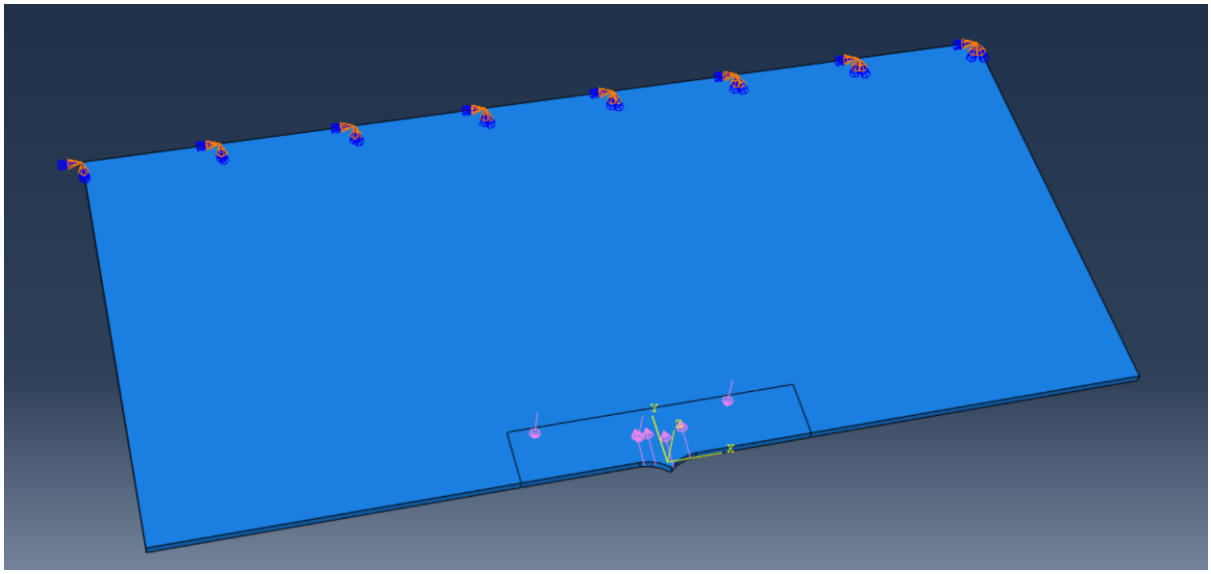

(a) Full view of the ice sheet

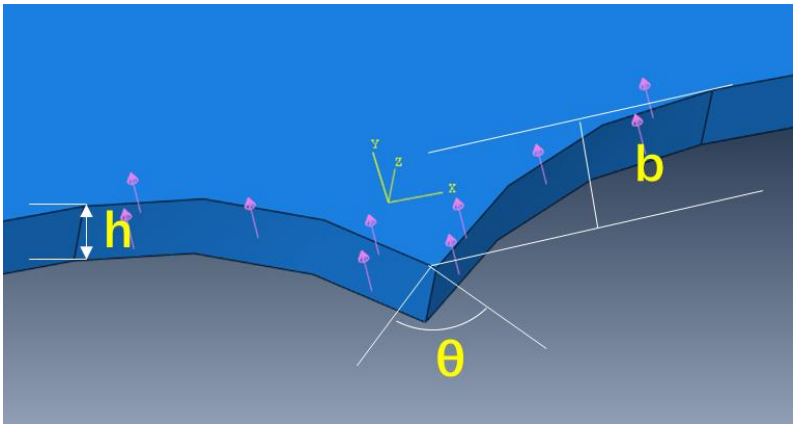

(b) Enlarged view of the ice wedge

Figure 1. The geometric model of the ice sheet

To obtain more general results, the ice wedge depth b is nondimensionalized with respect to the characteristic length l_c, and b/l_c is used as an input variable in this study.

Lu et al. (2015) pointed out that when the size of the ice cover exceeds $4l_c$, it can be considered as a semi-infinite ice cover, and the boundary effect on the loading region can be neglected. Therefore, in this study, the width of the ice cover is set to be $4l_c$, and the length is set to be $8l_c$.

During the interaction between the ship and the ice cover, the sea ice in the contact region undergoes crushing and spalling, breaking into fine fragments. However, there is currently no effective method to accurately model this fragmentation. Therefore, in this study, the failure of sea ice in the contact region is not considered.

As shown in Figure 2, the contact force acting on the contact surface is decomposed into two components: the out-of-plane force F_z (i.e., bending force) acting on the upper surface of the undeformed ice wedge, and the in-plane force F_y acting on the side surface. The friction force F_f also acts on the side surface.

The ship hull or structure interacting with the ice cover is idealized as an inclined rigid plate. The inclination of the hull is characterized by the tangent of the hull angle β, denoted as k, instead of using the angle itself. This choice facilitates the definition of the out-of-plane force F_z and the in-plane force F_y as independent parameters. This study aims to investigate the influence of various parameters on the stress within the ice layer during local ship-ice interaction. For simplicity, the out-of-plane load F_z is set as a constant value, while the magnitudes of the in-plane load F_{y} and frictional load F_{f} are defined as follows:

$$F_{\mathrm{y}} = F_y/k[\mathrm{N}/m^2] \tag{2}$$

$$F_f = f * F_z[\mathrm{N}/m^2] \tag{3}$$

Where f is the friction coefficient . And the direction of the friction force F_f is orthogonal to both the out-of-plane force F_z and the in-plane force F_y.

The penetration process of the ship hull into the ice wedge during interaction is simplified as the progression of the in-plane and out-of-plane loading regions along the surface of the ice wedge. The expansion velocities are v and $\frac{v}{k}$, respectively.

To reduce the number of parameters, the magnitude of the bending force F_z is set as a constant value in this study and is not treated as a variable of interest.

In summary, five parameters are used to describe the local interaction scenario between the ship and the ice cover: the nondimensionalized ice wedge depth b/l_c, the wedge angle θ, the tangent of the hull inclination angle k, the friction coefficient f, and the ship-ice interaction velocity v.

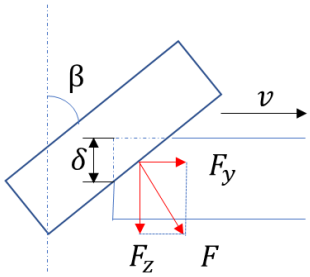

(a) Side view

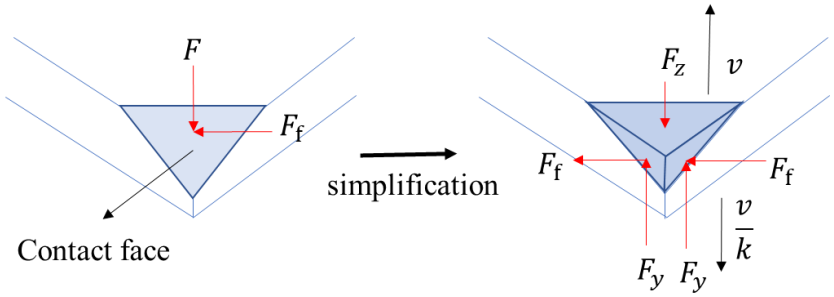

(b) Top view

Figure 2. Simplified schematic of the ship-ice contact force

Numerical simulation based on FEM

Finite Element Method (FEM) is employed to numerically investigate the influence of various parameters on the results. The simulations are performed using the dynamic implicit solver in ABAQUS/STANDARD, in order to account for the effects of dynamic response.

Regarding the influence of seawater during the ship-ice interaction process, Li et al. (2020) pointed out that the hydrodynamic effects of seawater can be neglected, and only the hydrostatic effect needs to be considered. Therefore, in this study, the effect of seawater on the ice cover can be simplified as an elastic foundation. The root of the ice cover is fully fixed to prevent any movement. A refined mesh region is applied near the ice wedge to ensure the accuracy of the results.

In the simulation, a vertical pressure load is applied on the upper surface of the sea ice. The in-plane force and friction force are combined into a surface traction load applied on the side surface of the ice wedge. ABAQUS's standard loading methods are limited to applying loads over fixed areas. However, in actual ship-ice interaction, the contact region propagates forward along the ice surface over time. Therefore, the loading area must dynamically change with time to realistically represent the movement of the contact zone.

To implement this, we developed custom user subroutines — DLOAD and UTRACLOAD — to control the load application region as a function of time. The spatial region where the in-plane load $F_z(\mathrm{y},\mathrm{t})$ is applied is determined by the position of the ship at each time step, defined by the ship-ice interaction velocity v:

$$F_z(\mathrm{y},\mathrm{t}) = \begin{cases} F_0, & y \le -b + v * t \\ 0, & otherwise \end{cases} \ [\mathrm{N}/m^2] \qquad (4)$$

Where F_0 is the constant load.

Similarly, the load application region for the side surface load $F_{\mathrm{y,f}}(\mathrm{y},\mathrm{z},\mathrm{t})$ is expressed as:

$$F_{\mathrm{y,f}}(\mathrm{y},\mathrm{z},\mathrm{t}) = \begin{cases} F_0/k, & y \le -b + v * t \ and \ z \ge h + \frac{y}{k} - \frac{v*t-b}{k} \\ 0, & otherwise \end{cases} \ [\mathrm{N}/m^2] \qquad (5)$$

Sensitivity analysis

The model was constructed using Fully Integrated Quadratic Hexahedral Elements (C3D20). Generally, reduced integration linear elements offer higher computational efficiency and are more widely used. However, reduced integration elements (C3D8R) exhibit lower accuracy, requiring enough layers in the ice thickness direction to ensure convergence of the results.

A greater number of layers results in an increased number of elements, which in turn leads to longer computation times. Figure 3 compares the computational results obtained using C3D20 elements with those using C3D8R elements with varying numbers of ice layers. It can be observed that as the number of layers increases, the results from the reduced integration elements gradually converge toward those obtained from the fully integrated elements.

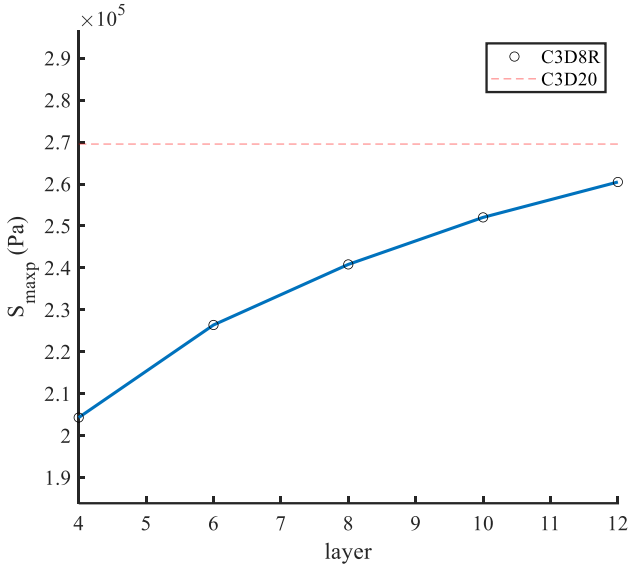

Figure 3 Sensitivity verification for different integration elements

Simulation conditions

In this study, the ship-ice interaction process is characterized by a set of parameters: the nondimensionalized ice wedge depth b/l_c, the wedge angle θ, the tangent of the hull inclination angle k, the friction coefficient f, and the ship-ice interaction velocity v. The range of values for these input parameters is summarized in Table 1.

Table 1 Input variables in simulation

Parameter	Range	Unit	Number
θ	[15, 30, 45, 60, 75, 90]	deg	6
b/l_c	[0.1, 0.2, 0.5, 1, 2]	–	5
k	[0.5, 0.75, 1, 1.5, 2]	–	5
v	[0.1, 1, 5]	m/s	3
f	[0.0, 0.05, 0.10, 0.15, 0.20, 0.25, 0.3]	–	7

The size and property parameters of the sea ice used in the simulation are shown in Table 2. Sea ice is modeled as a purely elastic material in the simulation. This is because this study does not focus on the plastic deformation and failure process of the ice. The properties of sea ice, including ice thickness h, elastic modulus E, and the applied load F_y, are set as fixed values in the simulation. In practical applications, scaling laws can be used to extend the results to more general cases.

Table 2 parameters in simulation

Parameter	Notation	Value	Unit
Ice thickness	h	1	m
Ice density	ρ_i	920	kg/m^3
Elastic modulus	E	5	Gpa
Water density	ρ_w	1025	kg/m^3
Out-of-plane pressure	F_0	1	Mpa

RESULTS AND ANALYSIS

Taking the simulation condition of $v = 1.0\,m/s$, $k = 2$, $b/lc = 1, \theta = 90^\circ$, and $f = 0.05$ as an example, Figure 4 illustrates the variation of the maximum principal stress distribution in the ice wedge over the loading time. It can be observed that in the early stage of loading, when the loading area is relatively small, the peak of the maximum principal stress is concentrated near the tip of the ice wedge, close to the edge of the loading region. The stress distribution at this stage resembles the results predicted by Nevel's narrow wedge model.

However, as the loading region penetrates deeper, approaching the bottom edge of the ice sheet, the peak of the maximum principal stress shifts toward both sides of the ice wedge. This indicates that Nevel's narrow wedge assumption does not fully capture the actual stress distribution in the ice wedge during real ship-ice interactions.

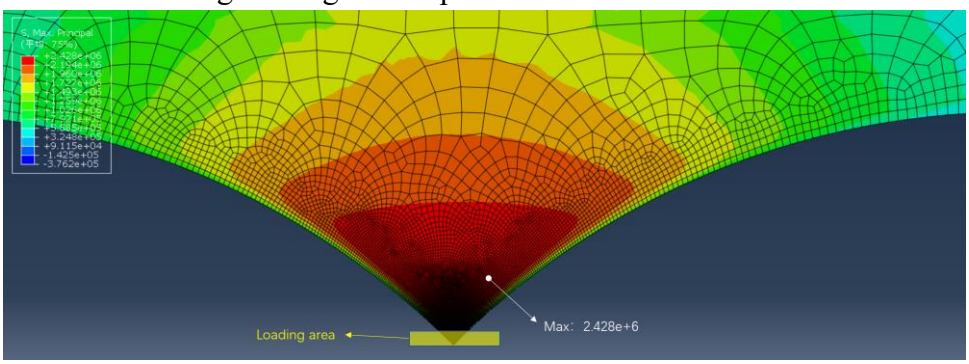

(a) $t = 1s$

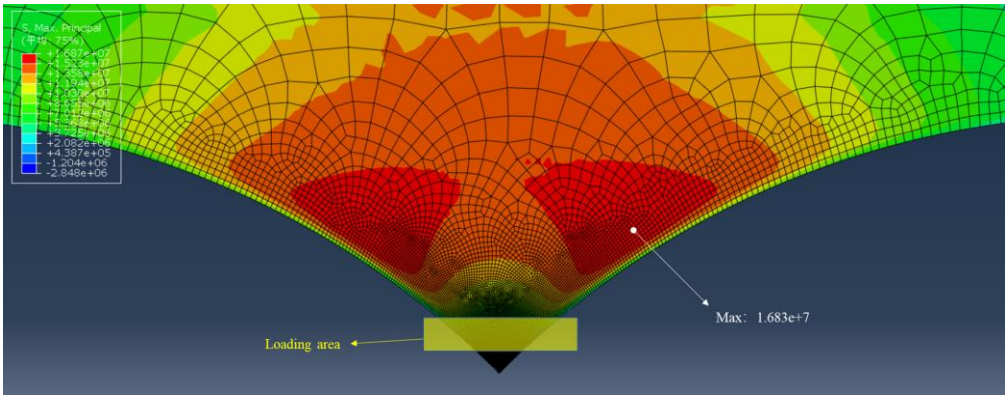

(b) $t = 3.2s$

Figure 4 Variation of the maximum principal stress distribution over loading time

Li et al. (2024) pointed out that when the stress in sea ice reaches the bending failure limit, additional energy is still required to fully fracture the ice. In this study, the fracture process from the failure threshold to complete breakage is not considered. Instead, the focus is placed on how different input parameters affect the stress distribution within the ice. Therefore, the bending strength of sea ice is not predefined, only the peak max_principal_stress S_{maxp} and its location under the given loading conditions are analyzed.

Considering that sea ice typically undergoes bending failure before the contact depth δ reaches the full ice thickness h, this study simulates only the interaction process up to a contact depth δ equal to ice thickness h.

Figure 5 shows the results of S_{maxp} under the influence of different parameters at a vertical contact depth of h. The effect of the friction coefficient f on the magnitude of S_{maxp} is approximately linear. This is reasonable, as the direction of the friction force is orthogonal to both the in-plane and out-of-plane forces, and thus does not directly influence the bending behavior of the ice sheet.

As the ice wedge depth b increases while other parameters remain constant, S_{maxp} increases in a power-law manner and gradually converges. This indicates that with increasing wedge depth, the influence of the ice sheet on the loading region near the wedge tip becomes less significant.

As the wedge angle θ increases, S_{maxp} increases in a power-law manner. This is because a larger wedge angle results in a wider ice wedge, which in turn leads to an increased contact area.

The influence of in-plane force F_x on S_{maxp} is also nonlinear. As the tangent value of the hull inclination angle k increases (i.e., indicating a decrease in the in-plane force), the peak maximum principal stress exhibits a nonlinear increase. This is because the presence of in-plane force restricts the vertical bending of the ice sheet, thereby reducing the stress experienced by the sea ice.

Furthermore, it can be observed that as the interaction velocity v increases, the S_{maxp} decreases. This suggests that with an increase in v, the ice sheet's bearing capacity increases. More specifically, it can be observed that at $v = 0.1m/s$ and $v = 1m/s$, the difference in

S_{maxp} is not significant. However, at $v = 5m/s$, the decrease in S_{maxp} is very pronounced. It can be inferred that dynamic effects during ship–ice interactions are not prominent at low velocities and can be treated as quasi-static loading. However, at high velocities, dynamic effects become significant, which may have been overlooked in previous studies.

However, the effect of v on the results in this study is not as pronounced as observed by Varsta (1983) in full-scale observations. The authors attribute this to two main factors. First, the viscoplastic behavior of sea ice is neglected in this study. Second, the loading region considered here is relatively small compared to the characteristic length of the ice. Kim et al (2022) conducted simulation studies on wedge-shaped beams with varying loading region lengths and loading velocities. Their results showed that when the loading region is smaller than $0.1lc$, dynamic effects are negligible. Dynamic effects become significant only when the loading region exceeds lc.

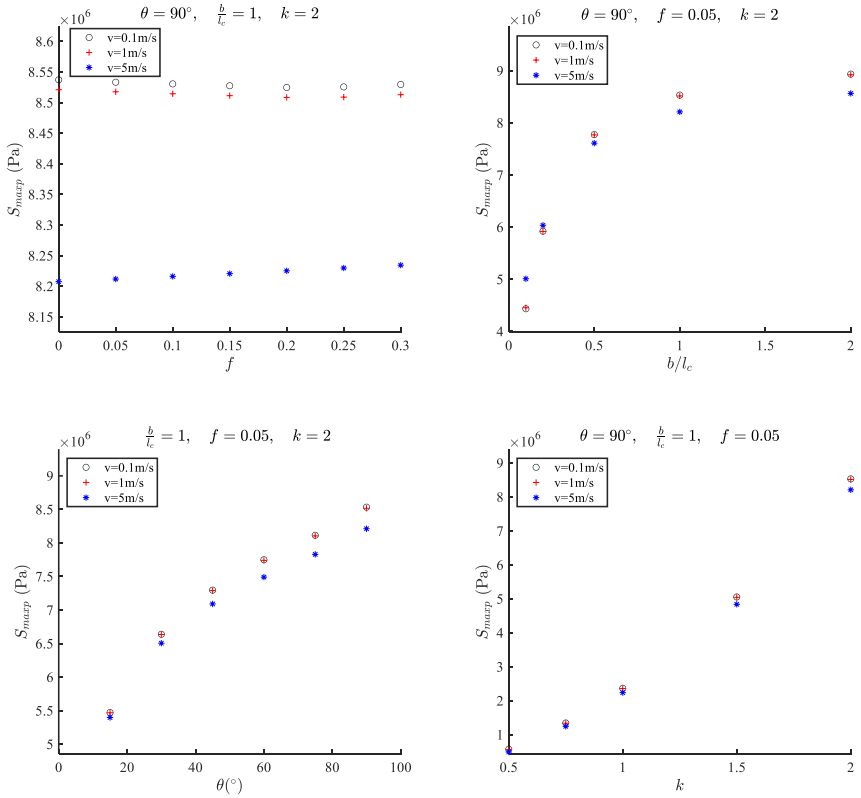

Figure 5 The S_{maxp} at the end of the simulation, as a function of f, b/l_c, θ, and k.

Figure 6 shows the time history curves of the S_{maxp} with different v and k. To compare the results at different velocities, the horizontal axis is represented by the loading displacement vt. It can be observed that as k increases, the difference in S_{maxp} between different v decreases. In other words, as the in-plane force decreases, the dynamic effects of the ship–ice interaction diminish. This implies that the presence of in-plane forces amplifies the dynamic effects during ship–ice interactions.

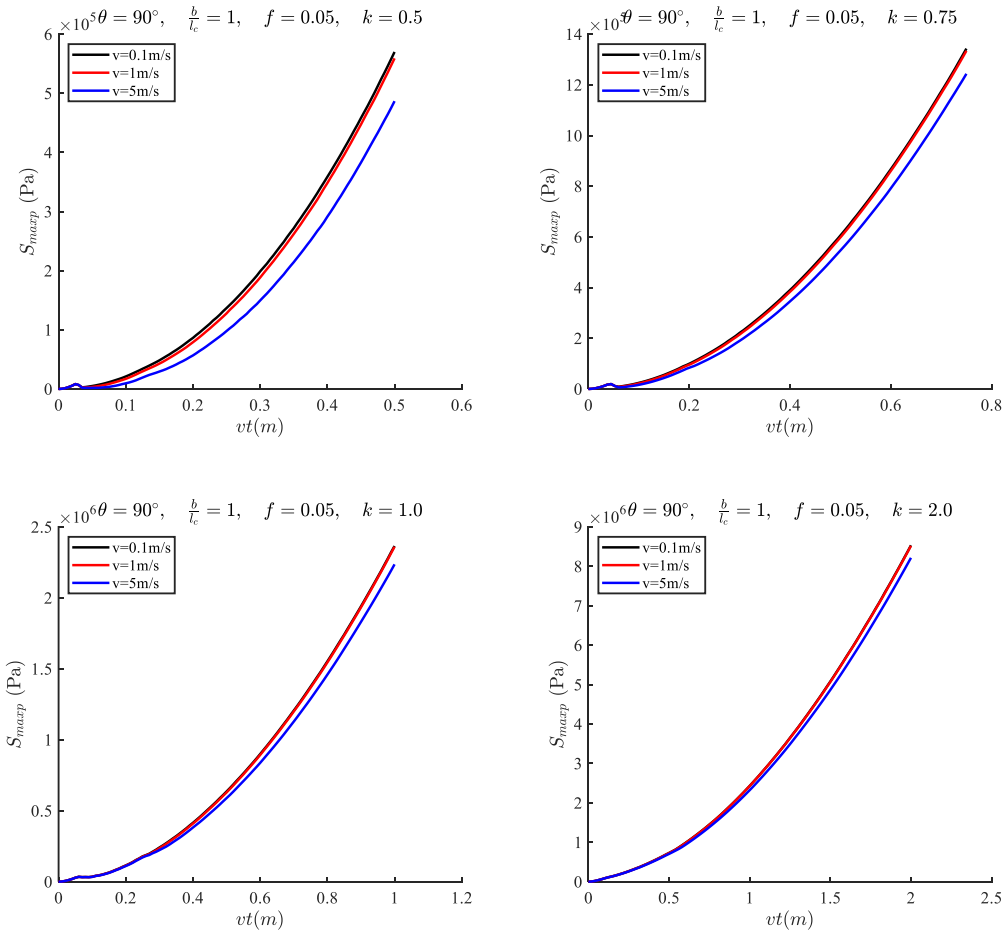

Figure 6 Time history curves of S_{maxp} with different v and k.

This study further investigates the relationship between the crack initiation location and various parameters during the bending failure of the ice sheet. The plastic failure process of sea ice is neglected, and the location of S_{maxp} is assumed to represent the crack initiation point. The distance l_b from the crack initiation location to the tip of the ice wedge is extracted and used as the crack length for the analysis. Figure 7 shows the results of l_b under different parameter conditions, at a vertical contact depth of h. To maintain generality, l_b is nondimensionalized with respect to the characteristic length of sea ice l_c.

It can be observed that the crack length l_b appears to be independent of the friction coefficient f. This is consistent with the previous analysis, as the direction of the friction force is orthogonal to both the in-plane and out-of-plane forces and does not affect the bending behavior of the ice sheet. Therefore, it does not influence the crack initiation location.

The relationship between crack length l_b and the ice wedge depth, wedge angle, and hull inclination angle seem to align with the relationship between S_{maxp} and these parameters. Moreover, under high-speed loading conditions, the crack length decreases.

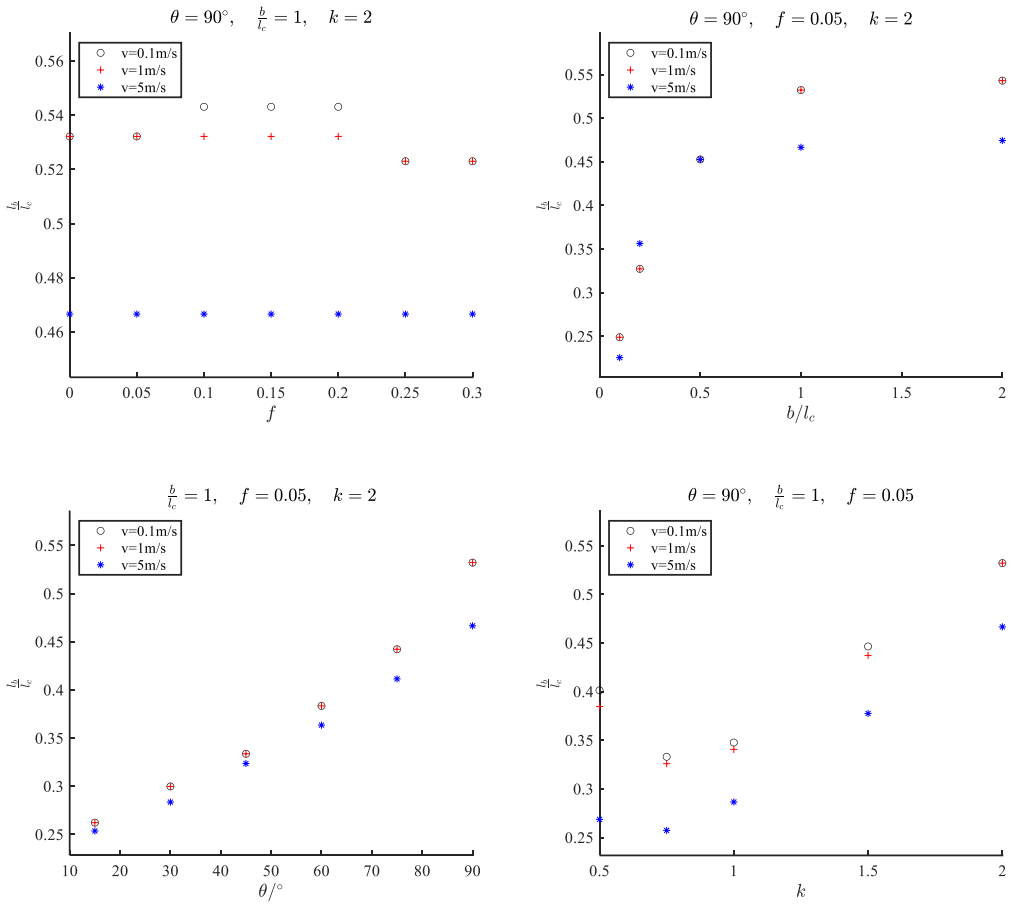

Figure 7 l_b/l_c at the end of the simulation, as a function of f, b/l_c, θ, and k.

Figure 8 shows the time history curves of the crack length under the influence of different v and k. It can be observed that as k increases (i.e., as the in-plane force decreases), the difference in crack length between different velocities becomes smaller. This is consistent with the previous analysis, where the presence of in-plane forces amplifies the dynamic effects during ship–ice interactions. Additionally, the crack length exhibits a "stepping" phenomenon as the loading position penetrates deeper.

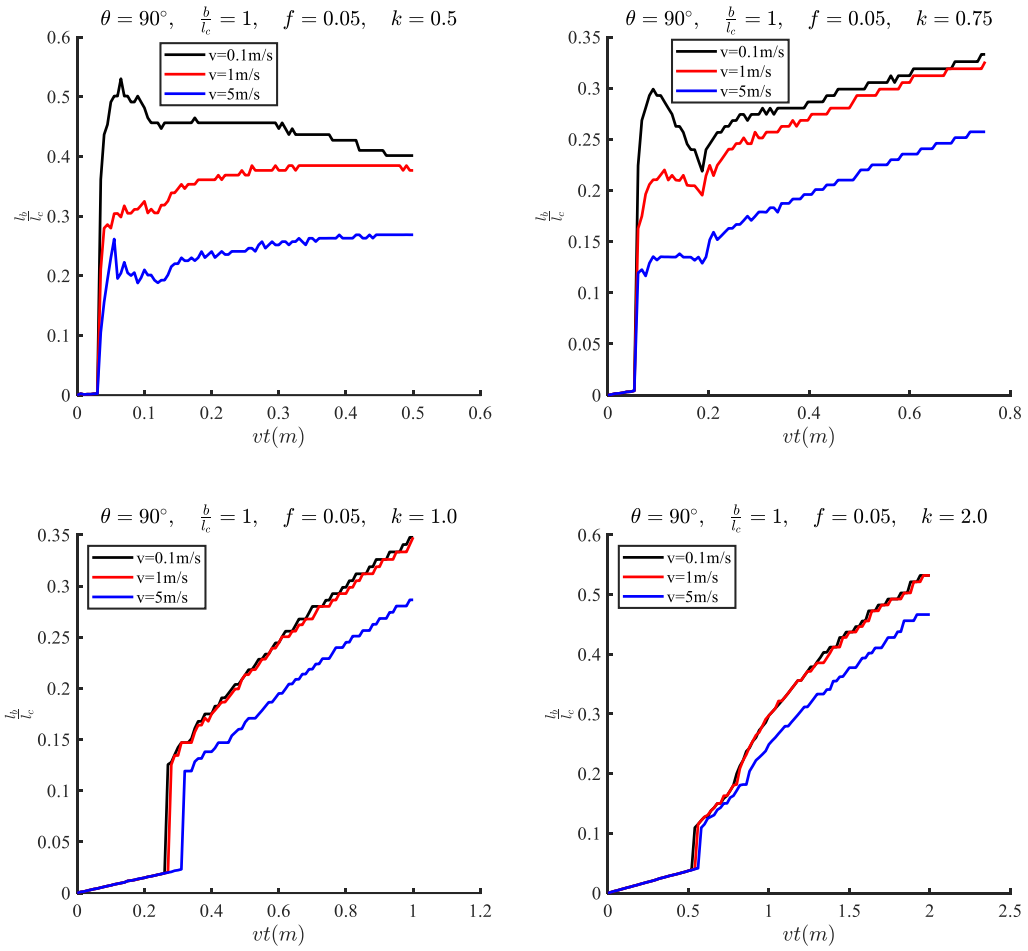

Figure 8 Time history curves of l_b/l_c with different v and k.

CONCLUSIONS

This study re-parameterizes the ship-ice interaction scenario using five key parameters: the nondimensionalized ice wedge depth b/l_c, the wedge angle θ, the tangent of the hull inclination angle k, the friction coefficient f, and the ship-ice interaction velocity v. Based on this framework, a finite element model of the ship-ice interaction is established. Based on FEM, this study investigates how these parameters influence the peak max_principal_stress S_{maxp} and crack length during the ship-ice interaction process. The implementation of a user-defined subroutine enabled time-dependent pressure loading, allowing for a more realistic simulation of the penetration process during local ship–ice interaction. In this study, the plastic failure process of sea ice is neglected. The location of S_{maxp} is assumed to represent the crack initiation point, and its distance from the tip of the ice wedge is considered as the crack length.

The results show that each parameter has a varying degree of impact on the stress experienced by the sea ice and its distribution. Due to the neglect of sea ice's viscoplasticity, the dynamic effects are not significant in the results. However, the trends in dynamic effects with respect to the parameters can still be observed.

Overall, the research model proposed in this study indicates that the actual ship-ice interaction is governed by a broader range of factors, providing valuable insights into the mechanisms of ship-ice interactions.

ACKNOWLEDGEMENTS

This study was supported by the Young Scientists Fund of National Natural Science Foundation of China (52301331), National Key Technologies Research and Development Program (Grant No. 2022YFE0107000), General Projects of National Natural Science Foundation of China (Grant No. 52171259), High-tech ship research project of Ministry of Industry and Information Technology ([2021]342), Science and Technology Commission of Shanghai Municipality Project (22DZ1204403, 23YF1419900), Foundation of State Key Laboratory of Ocean Engineering in Shanghai Jiao Tong University (GKZD010086-2).

REFERENCES

Kim J H, Lu W, Lubbad R, et al, 2022. Dynamic bending of an ice wedge resting on a winkler-type elastic foundation. *Cold Regions Science and Technology*, 199: 103579.

Kerr A D, 1976. The bearing capacity of floating ice plates subjected to static or quasi-static loads. *Journal of glaciology*, 17(76) , pp.229-268.

Li F, Chen J, Zhou L, et al, 2024. Investigation of ice wedge bearing capacity based on an anisotropic beam analogy. *Ocean Engineering*, 302: 117611.

Li F, Kotilainen M, Goerlandt F, et al, 2019. An extended ice failure model to improve the fidelity of icebreaking pattern in numerical simulation of ship performance in level ice. *Ocean Engineering*, 176, pp.169-183.

Li F, Kõrgesaar M, Kujala P, et al, 2020. Finite element based meta-modeling of ship-ice interaction at shoulder and midship areas for ship performance simulation. *Marine Structures*, 71: 102736.

Lindquist A, 1989. Straightforward method for calculation of ice resistance of ships. *POAC'89*.

Lubbad R, Løset S, 2011. A numerical model for real-time simulation of ship–ice interaction. *Cold Regions Science and Technology*, 65(2), pp.111-127.

Lu W, Lubbad R, Løset S, 2015. Out-of-plane failure of an ice floe: Radial-crack-initiation-controlled fracture. *Cold regions science and technology*, 119, pp.183-203.

Metrikin I, Løset S, 2013. Nonsmooth 3D discrete element simulation of a drillship in discontinuous ice, *Proceedings of the International Conference on Port and Ocean Engineering Under Arctic Conditions*.

Nevel D.E., 1961. The narrow free infinite wedge on an elastic foundation.

Riska K, 1997. *Performance of merchant vessels in ice in the Baltic*. Sjöfartsverket.

Varsta P, 1983. On the mechanics of ice load on ships in level ice in Baltic Sea.

Zhou L, Chuang Z, Ji C, 2018. Ice forces acting on towed ship in level ice with straight drift. Part I: Analysis of model test data. *International journal of naval architecture and ocean engineering*, 10(1), pp.60-68.